Stochastic dynamics of ϕ^4 kinks: numerics and analysis

Grant Lythe

School of Mathematics, University of Leeds, UK

Summary. Given a noise intensity or "temperature", the stationary density of the overdamped ϕ^4 SPDE corresponds to a mean number of kinks and antikinks that is maintained by a balance between nucleation of new kink-antikink pairs and annihilation whenever a kink and antikink collide. We consider numerical methods for solution of the SPDE, and a definition of the location of the centre of a kink using a smoothing function that is the derivative of the function describing the shape and energy of an isolated kink. This allows calculation of the diffusivity of a kink and defines the parameter characterising the "small-noise" régime. In the reaction-diffusion description of the dynamics (where kink-antikink pairs are nucleated with rate Γ, diffuse with diffusivity, D and annihilate on collision) the number of kinks per unit length in the steady-state has a simple exact expression.

1

Stochastic dynamics of ϕ^4 kinks: numerics and analysis

Main Abbreviations

○ ODE: Ordinary differential equation
○ SDE: Stochastic differential equation
○ SPDE: Stochastic partial differential equation
○ RHS: right hand side
○ LHS: left hand side

1 Introduction

Extended nonlinear systems often exhibit localized structures, such as moving domain walls, that move about under the influence of perturbations [1–6]. The ϕ^4 equation can be used in multiple dimensions [7,8], but we restrict ourselves to one space dimension, where the localised structures are known as kinks and antikinks [2]. Consider the stochastic partial differential equation for a field whose value at position $x \in [0, L]$ and time t is denoted $\boldsymbol{\Phi}_t(x)$ [9–19]:

$$\frac{\partial}{\partial t}\boldsymbol{\Phi}_t(x) - \frac{\partial^2}{\partial x^2}\boldsymbol{\Phi}_t(x) = \frac{1}{\alpha}(\boldsymbol{\Phi}_t(x) - \boldsymbol{\Phi}_t^3(x)) + (2KT)^{1/2}\,\boldsymbol{\eta}_t(x) \tag{1}$$

where the last term in (1) is space-time white noise [20–29]:

$$\mathbb{E}(\boldsymbol{\eta}_t(x)\boldsymbol{\eta}_{t'}(x')) = \delta(x - x')\delta(t - t'). \tag{2}$$

The dynamics can be thought of as that of a string subject to a double-well on-site potential (imagine two parallel trenches) and additive white noise all along its length. The amplitude of the noise is $(2KT)^{1/2}$ where T has the interpretation of temperature and K is Boltzmann's constant. We will use the notation $\beta = KT^{-1}$. The field $\boldsymbol{\Phi}_t$ is nondimensionalized in such a way that, on the RHS of (1), $\boldsymbol{\Phi}_t^3$ has the same coefficient as $\boldsymbol{\Phi}_t$. The distance x has been scaled so that the Laplacian term (second term on the LHS of (1)) has coefficient 1. The parameter α can be removed by rescaling time, but we retain it because several different conventions exist in the literature and because it provides a useful parameter (with dimensions

of time) in analytical calculations. In numerical work, we typically adopt $\alpha = 1$, use periodic boundary conditions on $[0, L]$ and take very large values of L.

An alternative notation to (1) is the following:

$$d\boldsymbol{\Phi}_t(x) = \frac{1}{\alpha}\left(\boldsymbol{\Phi}_t(x) - \boldsymbol{\Phi}_t^3(x) + \alpha\frac{\partial^2}{\partial x^2}\boldsymbol{\Phi}_t(x)\right)dt + (2KT)^{1/2}d\mathbf{B}_t(x),\qquad(3)$$

where

$$d\mathbf{B}_t(x)d\mathbf{B}_t(x') = \delta(x - x')dt.\qquad(4)$$

1.1 Some definitions

We may define the potential function

$$V(\boldsymbol{\Phi}) = \frac{1}{\alpha}(-\frac{1}{2}\boldsymbol{\Phi}^2 + \frac{1}{4}\boldsymbol{\Phi}^4),\qquad(5)$$

and the energy functional [30]

$$\mathcal{E}[f] = \int\left(V(f(x)) + \frac{1}{2}\left(\frac{\partial}{\partial x}f(x)\right)^2\right)dx.\qquad(6)$$

The kink shape function, $\phi(y)$, is defined as the solution of the ODE

$$\phi''(y) = V'(\phi(y)),\qquad \lim_{x\to-\infty}\phi(x) = -1 \text{ and } \lim_{x\to\infty}\phi(x) = 1.\qquad(7)$$

With $V(\boldsymbol{\Phi})$ as in (5), the solution of (7) is [31]

$$\phi(y) = \tanh(y/\sqrt{2\alpha}).\qquad(8)$$

(The function describing the shape of an antikink is $1 - \phi(y)$.) The energy or "mass" of a kink is

$$\begin{aligned}E_k = \mathcal{E}[\phi] &= \int_{-\infty}^{\infty}(V(\phi(y)) + \frac{1}{2}\phi'(y)^2)dy\\&= \int_{-\infty}^{\infty}\phi'(y)^2dy\\&= -\int_{-\infty}^{\infty}\phi''(y)\phi(y)dy\\&= \left(\frac{8}{9\alpha}\right)^{1/2}.\end{aligned}\qquad(9)$$

The ϕ^4 SPDE is primarily of interest in the "low noise" régime, where thye typical distance between kinks is much greater than the width of a kink. The square root of the ratio of the thermal energy KT and E_k is the corresponding small parameter:

$$\epsilon = \left(\frac{KT}{E_k}\right)^{\frac{1}{2}}.\qquad(10)$$

The notation (3) expresses, in a natural way, the simplest algorithm that may be used to solve the SPDE numerically [12,32,33]. Under finite differences, a numerical

solution is generated on a grid of points separated by Δx. That is, $x = i\Delta x$, $i = 1, \ldots, N$. The discretised version is a system of N SDEs:

$$\mathrm{d}\tilde{\boldsymbol{\Phi}}_t(i) = \frac{1}{\alpha}\left(-V'(\tilde{\boldsymbol{\Phi}}_t(i)) + \alpha\Delta x^{-2}\tilde{\Delta}\tilde{\boldsymbol{\Phi}}_t(i)\right)\mathrm{d}t + (2KT/\Delta x)^{1/2}\mathrm{d}\mathbf{W}_t(i), \qquad (11)$$

where

$$\tilde{\Delta}\tilde{\boldsymbol{\Phi}}_t(i) = \tilde{\boldsymbol{\Phi}}_t(i+1) + \tilde{\boldsymbol{\Phi}}_t(i-1) - 2\tilde{\boldsymbol{\Phi}}_t(i) \qquad \text{and} \qquad \mathbb{E}(\mathrm{d}\mathbf{W}_t(i)\mathrm{d}\mathbf{W}_t(i')) = \delta_{i-i'}\,\mathrm{d}t.$$

1.2 Structure of the Chapter

The ϕ^4 SPDE (1) can be solved as an initial value problem. On inspecting $\boldsymbol{\Phi}_t(x)$ as a function of x at a fixed t (that is, inspecting "configurations"), with $L \gg 1$, we observe wide regions where $\boldsymbol{\Phi}_t(x)$ is close to either 1 or -1, separated by narrow regions called kinks ($+1$ to the right) or antikinks ($+1$ to the left). These kinks and antikinks have some of the properties of particles: they are created in pairs, follow Brownian paths, and annihilate on collision. In the same way as the the series of configurations evolves towards a stationary density on the space of continuous functions, the number of kinks and antikinks per unit length evolves towards a well-defined mean value. As well as numerical methods for solving the SPDE itself, this Chapter will be concerned with extracting the density of kinks from the stationary density, with the practical question of how to locate the positions of kinks and antikinks in a configuration, with the question of the diffusivity of a kink, and with the rate of nucleation of kink-antikink pairs.

2 Stationary densities

The stationary density of the SPDE [34–40] is the limit as $\Delta x \to 0$ of the stationary density of the set of SDEs (11):

$$\rho(\Phi(1), \ldots, \Phi(N)) = Z_N \exp(-\beta\Delta x E(\Phi(1), \ldots \Phi(N))) \qquad (12)$$

where the energy function of the discretized system is,

$$E(\Phi(1), \ldots, \Phi(N)) = \sum_{i=1}^{N}\left(V(\Phi(i)) + \frac{\alpha}{2}\left(\frac{\Phi(i) - \Phi(i-1)}{\Delta x}\right)^2\right) \qquad (13)$$

and the partition function [41–43] is

$$Z_N = \int_{-\infty}^{\infty}\cdots\int_{-\infty}^{\infty}\exp(-\beta\Delta x E(\Phi(1), \ldots \Phi(N)))\mathrm{d}\Phi(1)\ldots\mathrm{d}\Phi(N). \qquad (14)$$

Using the "transfer integral" [10, 12, 42, 44, 45], it is possible to calculate Z_N in the continuum limit, $N \to \infty$ with $L = N\Delta x$ fixed:

$$Z = \lim_{N\to\infty} Z_N = \lim_{N\to\infty}\int_{-\infty}^{\infty}\cdots\int_{-\infty}^{\infty}\prod_{i=1}^{N}T(\Phi(i), \Phi(i+1))\mathrm{d}\Phi(1)\ldots\mathrm{d}\Phi(N), \qquad (15)$$

where

$$T(\Phi(i), \Phi(i+1)) = \exp\left(-\frac{1}{2}\beta\Delta x\left(\alpha\left(\frac{\Phi(i+1)-\Phi(i)}{\Delta x}\right)^2 + V(\Phi(i)) + V(\Phi(i+1))\right)\right)$$

and $\Phi(N+1) = \Phi(1)$. To proceed, suppose we can find a suitable set of eigenfunctions ψ_n and corresponding eigenvalues t_n satisfying

$$\int_{-\infty}^{\infty} T(\Phi(i), \Phi(i+1))\psi_n(\Phi(i))\mathrm{d}\Phi(i) = t_n\psi_n(\Phi(i+1)). \tag{16}$$

Then the integral in (15) is written as

$$Z_N = \int_{-\infty}^{\infty}\cdots\int_{-\infty}^{\infty}\prod_{i=1}^{N}\left(\sum_n t_n\psi_n(\Phi(i))\psi_n(\Phi(i+1))\right)\mathrm{d}\Phi(1)\ldots\mathrm{d}\Phi(N) = \sum_n t_n^N.$$

Now $Z = \lim_{N\to\infty}\sum_n t_n^N = t_0^N$, where t_0 is the maximum eigenvalue. The functions ψ_n are solutions of the well-known equation $[12, 46, 47]$

$$\left(-\frac{1}{2\alpha\beta^2}\frac{\partial^2}{\partial\Phi^2} + V(\Phi)\right)\psi_n = \epsilon_n\psi_n, \qquad \text{and } t_n = \mathrm{e}^{-\beta\Delta x\epsilon_n}. \tag{17}$$

Now we are in a position to use this information to calculate quantities of interest, such as long-time mean values of the field. The mean value of $f(\boldsymbol{\Phi}_t(x))$ as $t\to\infty$ is independent of x and given by

$$\lim_{t\to\infty}\mathbb{E}(f(\boldsymbol{\Phi}_t(x))) = \frac{1}{Z}\lim_{N\to\infty}\int_{-\infty}^{\infty}\cdots\int_{-\infty}^{\infty}f(\Phi(j))\prod_{i=1}^{N}T(\Phi(i), \Phi(i+1))\mathrm{d}\Phi(1)\ldots\mathrm{d}\Phi(N),$$

where $x = j\Delta x$. Thus

$$\lim_{t\to\infty}\mathbb{E}(f(\boldsymbol{\Phi}_t(x))) = \int_{-\infty}^{\infty}f(\Phi)\psi_0(\Phi)^2\mathrm{d}\Phi. \tag{18}$$

That is, the square of the zeroth eigenfunction of the transfer operator is the "one-point density function", which has peaks near ± 1 but is not simply related to $V(\Phi)$ [10]. Knowing the one-point density function permits fully nonlinear calculation of numerical values, for example of the mean value of $\boldsymbol{\Phi}_t(x)$, to arbitrary precision, for comparison with the results of direct simulation of the SPDEs [9, 11]. The results from the transfer integral depend only on β in the limit $\Delta x \to 0$. However, because the transfer integral is explicitly written with the form of the spatial discretisation, quantities such as the one-point density and correlation length can be calculated for finite Δx [12].

When kinks are the most interesting aspect of the system, the most illuminating consequence of the stationary density is the correlation function, which is the mean of the product of values at two different spatial points, as a function of their separation:

$$c(|x-y|) = \lim_{t\to\infty}\mathbb{E}(\boldsymbol{\Phi}_t(x)\boldsymbol{\Phi}_t(y))$$

$$= \frac{1}{Z}\lim_{N\to\infty}\int_{-\infty}^{\infty}\cdots\int_{-\infty}^{\infty}\Phi(k)\Phi(j)\prod_{i=1}^{N}T(\Phi(i), \Phi(i+1))\mathrm{d}\Phi(1)\ldots\mathrm{d}\Phi(N),$$

where $x = j\Delta x$ and $y = k\Delta x$. Thus the spatial correlation function is a sum of exponentials:

$$c(|x - y|) = t_0^{-|k-j|} \sum_n s_n^2 t_n^{|k-j|} = \sum_n s_n^2 \exp(-\beta x(\epsilon_n - \epsilon_0)). \tag{19}$$

The "correlation length" is given by

$$\lambda = -\lim_{x \to \infty} \frac{c(x)}{c'(x)} = \frac{1}{\beta(\epsilon_1 - \epsilon_0)}. \tag{20}$$

As $x \to \infty$, $c(x) \to s_1^2 \exp(-x/\lambda)$. If kinks and antikinks are randomly distributed in space, then the density of kinks is simply $1/(4\lambda)$ [9].

The existence of *exact* quantities that can be used to benchmark numerical results and analytical approximations is of immense value. For example, the correct values of λ can be evaluated to arbitrary precision by numerical solution of (17). For some choices of $V(\phi)$ and some parameter values, analytical results are known [48–50].

There is an interesting relations between the stationary density of an SPDE and the Markov chain Monte Carlo (MCMC) method in computational Bayesian statistics, which is a procedure for sampling by constructing a Markov process whose invariant density is equal to a target density [51]. The configurations (functions of space) making up the stationary density of the SPDE sample from the same density as the sample paths (functions of time) of a suitably-constructed SDE. In diffusion-bridge sampling, the required processes satisfy SPDEs of the form (1), having unique invariant measures that are ergodic [35, 52, 53].

3 Numerical solution

As the notation (11) suggests, in the Euler algorithm, the change between time t and time $t + \Delta t$ at spatial location i is

$$\tilde{\boldsymbol{\Phi}}_{t+\Delta t}(i) - \tilde{\boldsymbol{\Phi}}_t(i) = \left(-V'(\tilde{\boldsymbol{\Phi}}_t(i)) + \alpha \Delta x^{-2} \tilde{\Delta} \tilde{\boldsymbol{\Phi}}_t(i)\right) \frac{\Delta t}{\alpha} + \left(\frac{2KT}{\Delta x}\right)^{1/2} \Delta \mathbf{B}_t(i), \tag{21}$$

where $\Delta \mathbf{B}_t(i)$ is Gaussian random variable at each i and t with mean zero and

$$\mathbb{E}(\Delta \mathbf{B}_t(i) \Delta \mathbf{B}_{t'}(i')) = \begin{cases} \Delta t & i = i' \text{ and } t = t', \\ 0 & \text{otherwise .} \end{cases}$$

Perhaps the only counter-intuitive aspect of the algorithm is the scaling of the noise with Δx in (21).

It is straightforward to use the Heun algorithm instead of (21), so that errors in quantities such as the mean value at a spatial point are proportional to Δt^2 [10, 12]. In practice, an important part of designing a numerical experiment is choosing L, initial conditions, and run time [54]. The lower the temperature, the easier it is to identify and track kinks. However, genuine thermodynamic simulations with properly equilibrated kink populations require larger values of L, and longer run times, as larger values of β are chosen [9, 10].

An easier numerical task is to measure the diffusivity of an isolated kink: small spacetime domains lengths L can be used, with initial conditions chosen to have a single kink-antikink pair [55]. A consistent way to define and measure the position of (the centre of) a kink is then crucial. It is also possible to establish the rate of nucleation of new kink-antikink pairs by performing numerical experiments, with a kinkless initial configuration, at small and intermediate values of L [13].

It is a remarkable fact that the stationary density of the second-order-in-time SPDE

$$\frac{\partial^2}{\partial t^2}\boldsymbol{\Phi}_t(x) + \eta\frac{\partial}{\partial t}\boldsymbol{\Phi}_t(x) = \frac{\partial^2}{\partial x^2}\boldsymbol{\Phi}_t(x) + \frac{1}{\alpha}(\boldsymbol{\Phi}_t(x) - \boldsymbol{\Phi}_t^3(x)) + (2\eta KT)^{1/2}\,\boldsymbol{\eta}_t(x), \quad (22)$$

is independent of the damping η and identical to that of (1), although the dynamics depends strongly on η. Kink-antikink pairs do not necessarily annihilate on collision; they bounce inelastically, producing trapping and resonance phenomena [56] that are the analogues of breathers [57, 58] found in noiseless systems. A starting point for numerical solution of (22) could be to treat the system as $2N$ SDEs that can be solved using Euler or Heun timestepping. However, it is more efficient to use timestepping that explicitly respects the "partitioned" nature of the system (only half of the SDEs contain noise terms) [59–64]. "Leapfrog" [65, 66], "reverse leapfrog" [67] and "partitioned Runge-Kutta" [63] methods are available. The code used in the Chapter is reproduced in the Appendix.

4 Brownian motion of kinks

We cannot count kinks simply by counting zero crossings, because configurations are jagged on small scales. However, we can do so after convolving the configuration with a smoothing function [68]. Many symmetric functions with weight concentrated near zero could be used; here, we use the derivative of the function ϕ. That is, kinks and antikinks are located at values of x such that $h(x, \boldsymbol{\Phi}_t) = 0$ where

$$h(x, \boldsymbol{\Phi}_t) = \int \boldsymbol{\Phi}_t(u)\phi'(u - x)\mathrm{d}u. \quad (23)$$

If the position of a kink at tine t is $\mathbf{X}_t$ then the configuration in the vicinity of $\mathbf{X}_t$ region can be written as

$$\boldsymbol{\Phi}_t(x) = \phi(x - \mathbf{X}_t) + \boldsymbol{\chi}_t(x - \mathbf{X}_t). \quad (24)$$

By introducing the coordinate

$$y = x - \mathbf{X}_t, \quad (25)$$

the field $\boldsymbol{\chi}_t$ has stationary statistical properties [55, 68]. The separation (24) has been introduced by several authors [69, 70] and the assumption made that $\boldsymbol{\chi}_t(y)$ is "small" in a sense that we can now make precise, using the parameter ϵ defined in (10). The choice of the smoothing function in (23) is illustrated in Figure 1.

We proceed to derive an SDE for the evolution of the kink position. The general form for such an SDE is as follows [31]:

$$\mathrm{d}\mathbf{X}_t = a(\boldsymbol{\Phi}_t, t)\mathrm{d}t + b(\boldsymbol{\Phi}_t, t)\mathrm{d}\mathbf{W}_t^{(X)}. \quad (26)$$

Fig. 1. Top: a configuration from one numerical realisation. Bottom: zoomed-in views of two small regions, containing a kink and an antikink. The green line is the function $h(x, \boldsymbol{\Phi}_t)$, obtained using the smoothing function $\phi'(y)$. The parameters are $\alpha = 1$ and $\beta = 20$, the numerical simulation was carried out with $\Delta x = 0.1$ and $\Delta t = 0.002$

We have chosen to define the kink's position $\mathbf{X}_t$ by the condition

$$\int_{-\infty}^{\infty} \boldsymbol{\Phi}_t(x)\phi'(x - \mathbf{X}_t)\mathrm{d}x = 0. \tag{27}$$

Similarly, $\mathbf{X}_{t+\Delta t}$ is the value of x such that $h(x, \boldsymbol{\Phi}_{t+\Delta t}) = 0$. That is

$$\int_{-\infty}^{\infty} (\boldsymbol{\Phi}_t(x) + \Delta\boldsymbol{\Phi}_t(x))\phi'(x - \mathbf{X}_{t+\Delta t})\mathrm{d}x = 0, \tag{28}$$

where $\Delta\boldsymbol{\Phi}_t(x) = \boldsymbol{\Phi}_{t+\Delta t}(x) - \boldsymbol{\Phi}_t(x)$. Letting $\Delta t \to 0$, we can restate (28) in the form of a stochastic differential:

$$\mathrm{d}h(\mathbf{X}_t, \boldsymbol{\Phi}_t) = 0. \tag{29}$$

The Ito formula [71, 72] is used to expand (29), using (3) and (26):

$$\begin{aligned}
0 = & \int_{-\infty}^{\infty} \left(\mathrm{d}\boldsymbol{\Phi}_t(x)\phi'(x - \mathbf{X}_t)\right)\mathrm{d}x \\
& - \left(\int_{-\infty}^{\infty} \phi''(x - \mathbf{X}_t)\boldsymbol{\Phi}_t(x)\mathrm{d}x\right)\mathrm{d}\mathbf{X}_t \\
& + \left(\int_{-\infty}^{\infty} \phi'''(x - \mathbf{X}_t)\boldsymbol{\Phi}_t(x)\mathrm{d}x\right)\frac{1}{2}b^2(\boldsymbol{\Phi}_t)\mathrm{d}t \\
& - \int_{-\infty}^{\infty} ((2KT)^{1/2}b(t, \boldsymbol{\Phi}_t)\mathrm{d}\mathbf{W}_t^{(X)}\mathrm{d}\mathbf{B}_t(x)\phi''(x - \mathbf{X}_t))\mathrm{d}x.
\end{aligned} \tag{30}$$

The second term on the RHS of (30) is $\mathbf{M}_t\mathrm{d}\mathbf{X}_t$ where, using (24) and (9),

$$\mathbf{M}_t = -\int_{-\infty}^{\infty} \phi''(x - \mathbf{X}_t)\boldsymbol{\Phi}_t(x)\mathrm{d}x = E_\mathrm{k} + \int_{-\infty}^{\infty} \phi''(x - \mathbf{X}_t)\boldsymbol{\chi}_t(x)\mathrm{d}x. \tag{31}$$

Thus we find, performing the integral in the first term on the RHS of (30),

$$b(\boldsymbol{\Phi}_t, t) = \mathbf{M}_t^{-1}(2KTE_\mathrm{k})^{1/2}. \tag{32}$$

Thus, at lowest order in ϵ (10), $\mathbf{M}_t = E_\mathrm{k}$ and an isolated kink's motion is Brownian with diffusivity ϵ^2, that is, with mean-squared displacement at time t given by $2\epsilon^2 t$.

In order to calculate higher-order terms, we use the operator $\mathcal{L}$ that acts on a function $f(y)$ as follows

$$\mathcal{L}f(y) = \alpha f''(y) + f(y) - 3\phi^2(y)f(y). \tag{33}$$

The operator $\mathcal{L}$ is obtained from the equation of motion (1) by linearizing about the single-kink solution $\phi(y)$ [2]. The eigenvalue equation,
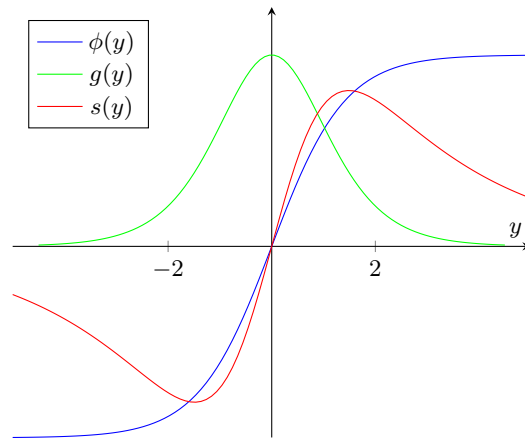
$$\mathcal{L}f(y) = -\lambda f(y), \tag{34}$$

has two discrete solutions and also has an infinite series of solutions with $\lambda > 2$. The discrete solutions [2]

$$g(y) = \sqrt{2\alpha}\phi'(y) = \frac{1}{\cosh^2(y/\sqrt{2\alpha})} \tag{35}$$

and

$$s(y) = \left(-\alpha\phi''(y)\phi(y)\right)^{1/2} = \frac{\sinh(y/\sqrt{2\alpha})}{\cosh^2(y/\sqrt{2\alpha})}, \tag{36}$$

known as the "translation mode" and "shape mode" [73], are plotted in Figure 2. $\mathcal{L}g(y) = 0$ and $\mathcal{L}s(y) = -\frac{3}{2}s(y)$. The eigenfunctions with $\lambda > 2$ are extended or "phonon" modes.

Fig. 2. The kink shape function, $\phi(y)$, is shown in blue. Also shown are the functions $g(y)$ and $s(y)$, eigenfunctions of the operator $\mathcal{L}$ with eigenvalues 0 and $-\frac{3}{2}$. $\alpha = 1$.

The inhomogeneous stochastic field $\boldsymbol{\chi}_t(y)$ may now be decomposed using the eigenfunctions of $\mathcal{L}$. As $t \to \infty$, at first order in ϵ, $\boldsymbol{\chi}_t(y)$ is Gaussian with mean zero; the amplitudes of the extended modes are independent Ornstein-Uhlenbeck processes with variance proportional to ϵ^2. At second order, the mean amplitude of the shape mode is nonzero. So too is the antisymmetric part of every second extended mode. Exchange of energy between these modes adds terms proportional to ϵ^2 to the diffusivity of a kink.

5 Nucleation of kink-antikink pairs

New kinks and antikinks never appear alone, but are created in pairs in "nucleation" events, when a fluctuation causes part of a configuration to surmount the energy barrier separating the two wells at -1 and $+1$. Similarly, kinks and antikinks disappear

in pairs, when their Brownian wanderings intersect. How frequent are nucleation events? We seek the rate Γ of nucleation events, per unit length and time.

It is possible, in principle, to calculate the rate of occurrence, per unit length in a large system, of fluctuations large enough to provoke nucleation [74, 75]. Intuitively, the rate should be proportional to $\exp(-2\alpha\beta E_k)$ because the nucleation event results in the creation of two localised structures, each with energy E_k [9, 74, 76–83]. Alternatively, it is illuminating to consider the balance between nucleation and annihilation events:

$$\Gamma\tau = \rho_k, \tag{37}$$

where τ is the mean lifetime of a kink and ρ_k is the number of kinks per unit length. The RHS of (37) is known from the stationary density of the SPDE and the transfer integral that allows the correlation length to be evaluated (Section 2): $\rho_k \propto \exp(-\alpha\beta E_k)$. The mean lifetime τ can be calculated by considering the life histories of kinks and antikinks, created in pairs and then diffusing until colliding and annihilating [84–88]. The diffusivity D is also well understood (Section 4). If the kink-antikink separation at the time of nucleation, b, is independent of β and much smaller than the typical distance between nearest-neighbour kinks and antikinks, then then most annihilation events are, in fact, recombination events between kink-antikink pairs that were nucleated together [9, 84]. Exact expressions exist for this diffusion-limited reaction scenario. The steady-state density in terms of the parameters Γ, D and b is given by [87]

$$\rho_k \to \left(\frac{b\Gamma}{2D}\right)^{1/2} \quad \text{as} \quad \left(\frac{2\Gamma}{D}\right)^{1/3} b \to 0.$$

Thus, because the steady-state density of kinks is proportional to $\exp(-\alpha\beta E_k)$, we conclude that the nucleation rate of kink-antikink pairs is proportional to $\exp(-2\alpha\beta E_k)$, consistent with intuition. Independently, the appropriate value for the parameter b has been estimated, from first-passage type numerical experiments on small-to-intermediate-sized domains, as $8\alpha E_k$ [13]. It is also possible to perform numerical experiments to evaluate the nucleation rate directly, as a function of β, to measure kink lifetimes and to distinguish recombinant and non-recombinant annihilation events [9].

Numerical experiments on large domains and over long times, while maintaining accurate spatial and temporal resolution, were only possible on computer clusters 10-20 years ago [9, 89] but are more accessible to desktop experiments nowadays. An example is given in Figure 3, where numerical counts of numbers of kinks per unit length are compared with the predictions obtained using (20). The larger the value of β, the smaller the steady-state number of kinks per unit length, and the longer the equilibration time.

6 Discussion

On the one hand, it is indispensable to perform numerical simulations of a detailed model of a physical system, on the largest domain and with the highest spatial resolution feasible, for as long a time as possible. Such numerical work is complemented by developing theoretical methods that efficiently identify the structures of interest and predict their number, form, dynamics and interactions. Some questions
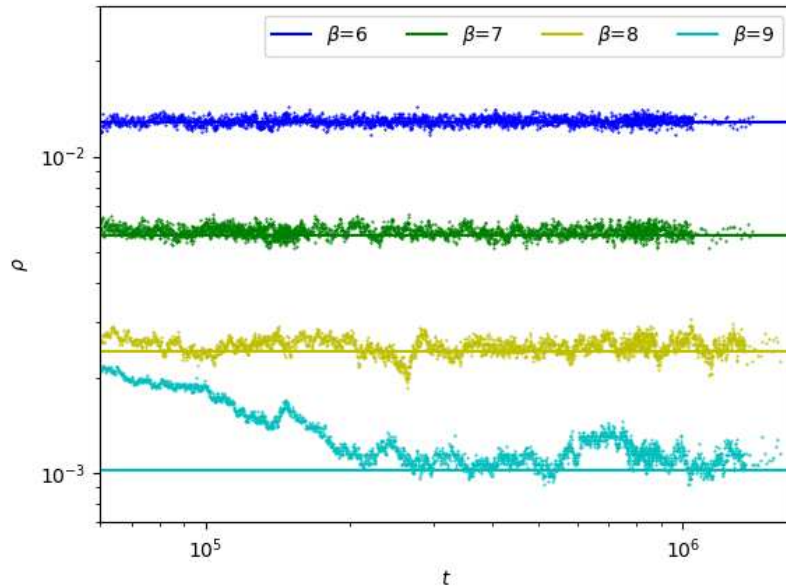
Fig. 3. Density of kinks versus time at different values of β. The solid lines are the predictions using (20). Dotted lines are numerical solutions with $\alpha = 1$, $\Delta x = 0.4$ and $\Delta t = 0.032$.

one can ask are: How many coherent structures are there, on average, in the long term? How do they move and interact with their environment and with each other? How strongly do these properties answers depend on parameters such as the temperature? In such circumstances, exact theoretical results are extremely valuable as benchmarks for numerical algorithms.

On the other hand, many theoretical results are approximations whose accuracy increases as the temperature decreases. However, low temperatures require large amounts of computer time because the timescales of the system typically increase as temperature decreases (so one must perform runs of increasing duration to sample adequately) and because the density of coherent structures also decreases with decreasing temperature (so larger systems are needed). Often, even a small decrease in temperature results in an order-of-magnitude increase in computing time required. The continuing increase in computing power available year by year, impressive though it is, will not be sufficient to break new ground without the assistance of new theoretical insights and new numerical methods.

Understanding of the noisy ϕ^4 equation in multiple space dimensions [7, 90, 91] is advancing. There are surely many interesting dynamical features of coherent structures in two and three space dimensions waiting to be discovered. Systems with multiplicative noise [92] tend to exhibit intermittent behaviours that are challenging for the theorist, numericist and physicist.

Acknowledgements

References

1. A. C. Scott, F. Chu and D. McLaughlin Proceedings IEEE **61**, 1443 (1973)
2. A. Bishop, J. Krumhansl and J. Schrieffer Physica D **1**, 1 (1980)
3. A. Sánchez and A. Bishop SIAM Review **40**, 579 (1998)
4. M. J. Ward Studies in Applied Mathematics **91**, 51 (1994)
5. T. Dauxois and M. Peyrard *Physics of Solitons* (Cambridge University Press) (2006)
6. J. García-Ojalvo and J. Sancho *Noise in spatially extended systems* (Springer Science & Business Media) (2012)
7. M. D. Ryser, N. Nigam and P. F. Tupper Journal of Computational Physics **231**, 2537 (2012)
8. J.-C. Mourrat and H. Weber Communications on Pure and Applied Mathematics **70**, 717 (2017)
9. S. Habib and G. Lythe Physical Review Letters **84**, 1070 (2000)
10. G. Lythe and S. Habib Computer Physics Communications **142**, 29 (2001)
11. G. Lythe and S. Habib Computing in Science and Engineering **8**, 10 (2006)
12. L. Bettencourt, S. Habib and G. Lythe Physical Review D **60**, 105039 (1999)
13. M. Castro and G. Lythe SIAM Journal on Applied Dynamical Systems **7**, 207 (2008)
14. T. Shardlow Electronic Journal of Differential Equations **47**, 1 (2000)
15. R. V. Kohn, F. Otto, M. G. Reznikoff and E. Vanden-Eijnden Communications on Pure and Applied Mathematics **LIX**, 0001 (2006)
16. M. A. Katsoulakis, G. T. Kossioris and O. Lakkis Interfaces and Free Boundaries **9**, 1 (2007)
17. M. A. Katsoulakis, G. T. Kossioris and O. Lakkis Interfaces and Free Bundaries **9**, 1 (2007)
18. F. Barret, A. Bovier, S. Méléard *et al.* Electronic Journal of Probability **15**, 323 (2009)
19. G. J. Lord, C. E. Powell and T. Shardlow *An introduction to computational stochastic PDEs* (Cambridge University Press) (2014)
20. J. Walsh in *Ecole d'été de probabilités de St-Flour XIV* (edited by P.L.Hennequin) (1986) 266–439
21. C. R. Doering Communications in Mathematical Physics **109**, 537 (1987)
22. T. Funaki Nagoya Mathematical Journal **89**, 129 (1983)
23. H. Kunita *Stochastic flows and stochastic differential equations* (Cambridge University Press) (1997)
24. G. D. Prato and J. Zabczyk *Stochastic Equations in Infinite Dimensions* (Cambridge University Press) (1992)
25. C. Prévôt and M. Röckner *A concise course on stochastic partial differential equations* (Springer) (2007)

26. A. Jentzen and P. E. Kloeden Proceedings of the Royal Society A: Mathematical, Physical and Engineering Science **465**, 649 (2009)
27. A. Jentzen and P. E. Kloeden *Taylor approximations for stochastic partial differential equations* (SIAM) (2011)
28. P. E. Kloeden, G. Lord, A. Neuenkirch and T. Shardlow Journal of Computational and Applied Mathematics **235**, 1245 (2011)
29. D. Khoshnevisan *Analysis of stochastic partial differential equations* volume 119 (American Mathematical Soc.) (2014)
30. W. Faris and G. Jona-Lasinio Journal of Physics A **15**, 3025 (1982)
31. T. Funaki Probability Theory and Related Fields **102**, 221 (1995)
32. I. Gyongy Potential Analysis **9**, 1 (1998)
33. I. Gyongy Potential Analysis **11**, 1 (1999)
34. M. Büttiker and R. Landauer Journal of Physics C **13**, L325 (1980)
35. A. Stuart, J. Voss and P. Wiberg Communications in Mathematical Sciences **2**, 585 (2004)
36. M. G. Reznikoff and E. Vanden-Eijnden ComptesRendus Academy Sciences Paris **1340**, 305 (2005)
37. H. Weber Communications on Pure and Applied Mathematics **63**, 1071 (2010)
38. A. Abdulle, G. Vilmart, K. Zygalakis *et al.* High order numerical approximation of the invariant measure of ergodic sdes (2013) mATHICSE Technical Report Nr. 27.2013, EPFL, Lausanne, Switzerland
39. M. Tretyakov and Z. Zhang SIAM Journal on Numerical Analysis **51**, 3135 (2013)
40. F. Otto, H. Weber, M. G. Westdickenberg *et al.* Electron. J. Probab **19**, 1 (2014)
41. A. Seeger and P. Schiller in *Physical Acoustics: Principles and Methods* (edited by W. P. Mason) (Academic press) (1966) 361–495
42. D. Scalapino, M. Sears and R. Ferrell Physical Review B **6**, 3409 (1972)
43. F. J. Alexander and S. Habib Physical Review Letters **71**, 955 (1993)
44. G. Parisi *Statistical Field Theory* (Addison-Wesley) (1988)
45. M. Creutz *Quarks, Gluons, and Lattices* (Cambridge University Press) (1)
46. J. Currie, J. Krumhansl, A. Bishop and S. Trullinger Physical Review B **22**, 477 (1980)
47. G. Lythe and S. Habib in *Proceedings of the IUTAM symposium on Nonlinear Stochastic Dynamics* (edited by N. Namachchivaya and Y.K.Lin) (Kluwer) (2003) 435–444
48. A. Khare, S. Habib and A. Saxena Physical Review Letters **79**, 3797 (1997)
49. A. Saxena and S. Habib Physica D **107**, 338 (1997)
50. S. Habib, A. Khare and A. Saxena Physica D **123**, 341 (1998)
51. W. Gilks, S. Richardson and D. Spiegelhalter, eds. *Markov Chain Monte Carlo in practice* (Chapman and Hall/CRC) (1996)
52. M. Hairer, A. Stuart, J. Voss and P. Wiberg Communications in Mathematical Sciences **3**, 587 (2005)
53. A. Apte, M. Hairer, A. Stuart and J. Voss Physica D **230**, 50 (2007)
54. R. D. Skeel Journal of Numerical Analysis, Industrial and Applied Mathematics **5**, 103 (2010)
55. G. Lythe and F. Mertens Physical Review E **67**, 027601 (2003)
56. D. K. Campbell, J. F. Schonfeld and C. A. Wingate Physica D: Nonlinear Phenomena **9**, 1 (1983)
57. H. Segur and M. D. Kruskal Physical Review Letters **58**, 747 (1987)

58. P. Kevrekidis, A. Saxena and A. Bishop Physical Review E **64**, 026613 (2001)
59. W. Wang and R. D. Skeel Molecular Physics **101**, 2149 (2003)
60. H. Schurz Stochastic Analysis and Applications **17**, 463 (1999)
61. H. Schurz in *Handbook of Stochastic Analysis and Applications* (edited by D. Kannan and V. Lakshmikantham) (Marcel Dekker) (2002) 237–359
62. B. Leimkuhler and S. Reich *Simulating Hamiltonian dynamics* (Cambridge University Press) (2004)
63. K. Burrage and G. Lythe SIAM Journal on Numerical Analysis **47**, 1601 (2009)
64. J. Voss Communications in Mathematical Sciences **10**, 1143 (2012)
65. R. Mannella Physical Review E **69**, 041107 (2004)
66. R. Mannella SIAM Journal on Scientific Computing **27**, 2121 (2006)
67. K. Burrage, I. Lenane and G. Lythe SIAM Journal on Scientific Computing **29**, 245 (2007)
68. D. Kaup Physical Review B **27**, 6787 (1983)
69. E. Tomboulis Physical Review D **12**, 1678 (1975)
70. H. Segur Journal of Mathematical Physics **24**, 1439 (1983)
71. C. W. Gardiner *Handbook of Stochastic Methods for Physics, Chemistry and the Natural Sciences* (Springer) third edition (2004)
72. S. Karlin and H. M. Taylor *A second course in stochastic processes* (Academic) (1981)
73. Y. S. Kivshar, D. E. Pelinovsky, T. Cretegny and M. Peyrard Physical Review Letters **80**, 5032 (1998)
74. M. Büttiker and R. Landauer Physical Review Letters **43**, 1453 (1979)
75. F. Barret *et al.* in *Annales de l'Institut Henri Poincaré, Probabilités et Statistiques* (Institut Henri Poincaré) (2015) volume 51 129–166
76. R. Landauer and J. Swanson Physical Review **121**, 1668 (1961)
77. J. Lothe and J. P. Hirth Physical Review **115**, 543 (1959)
78. M. Büttiker and R. Landauer Physical Review A **23**, 1397 (1981)
79. M. Büttiker and T. Christen Physical Review Letters **75**, 1895 (1995)
80. R. S. Maier and D. L. Stein Physical Review Letters **87**, 270601 (2001)
81. W. E, W. Ren and E. Vanden-Eijnden Communications on Pure and Applied Mathematics **LVII**, 0637 (2004)
82. R. V. Kohn, M. G. Reznikoff and Y. Tonegawa Calculus of Variations **25**, 503 (2006)
83. N. Berglund and B. Gentz Journal of Physics A: Mathematical and Theoretical **42**, 052001 (2009)
84. T. Christen and M. Büttiker Physical Review E **58**, 1533 (1998)
85. S. Habib, K. Lindenberg, G. Lythe and C. Molina-París Journal of Chemical Physics **115**, 73 (2001)
86. T. O. Masser and D. ben Avraham Physical Review E **63**, 006108 (2001)
87. G. Lythe Physica D **222**, 159 (2006)
88. H. C. Fogedby, J. Hertz and A. Svane Europhysics Letters **62**, 795 (2003)
89. F. J. Alexander, S. Habib and A. Kovner Physical Review E **48**, 4284 (1993)
90. M. Hairer, M. D. Ryser and H. Weber Electronis Journal of Probability **17**, 1 (2012)
91. J.-C. Mourrat and H. Weber The Annals of Probability **45**, 2398 (2017)
92. D. Khoshnevisan, K. Kim and Y. Xiao Communications in Mathematical Physics **360**, 307 (2018)

Appendix: python code

```python
#   GDL  2018.  python  3
#  Phi4  SPDE  with  (additive)  spacetime  white  noise
#  Measure  <phi>  and  correlation  function.
#  Count  kinks  using  smoothing  function  h(x).
#    example  command  lines
#    i)  to  start  from  t=0:
#    python  Count06.py  50000  100000  0.2  0.01  10.0
#    ii)  to  start  from  written  configuration:
#    python  Count06.py  Config10_20_10_100.dat  10000
import numpy as np
import os, sys

if len(sys.argv) ==6:
    # start from t=0
    N,tmax = int(sys.argv[1]),float(sys.argv[2])
    dx,dt = float(sys.argv[3]),float(sys.argv[4])
    beta = float(sys.argv[5])
    t = 0.0
    tstart = min(tmax/2,1000)
    phi = np.zeros(N)
else:
    # start from existing file
    startfile = open(sys.argv[1],'r')
    print(len(sys.argv))
    items = sys.argv[1].split('_')
    print(items)
    dx,dt = int(items[2])*0.01,int(items[3])*0.0001
    beta = float(items[0].replace('Config',''))
    t = int(items[4].split('.')[0])*1000.0
    tmax = t + float(sys.argv[2])
    print(dx,dt,beta,t,tmax)
    for line in startfile:
        oldconfig = line.split()
    phi = np.array([float(p) for p in oldconfig])
    N = len(phi)
    tstart = t

tint = max((tmax/1000),100)
k,fac,nc = 1.0/(dx*dx),np.sqrt(2*dt/(beta*dx)),int(100/dx)

def phicub(ph):
    ''' cube of phi '''
    return ph*ph*ph

def lap2(phi):
    ''' laplacian of phi '''
    return np.append(phi[1:], phi[0]) + np.append(phi[-1], phi[:-1]) - 2*phi

def myra2(N, mysd):
    ''' N draws from gaussian distribution '''
    return np.random.normal(0,mysd,N)

def euler(phi,g,dt,k):
    ''' one Euler step '''
    return phi + dt*(phi-phicub(phi)+k*lap(phi)) + g

def heun2(phi,g,dt,k):
    ''' one Heun step, keep intermediate to avoid recalculation '''
    phit = phi.copy()
    pinc = phi - phicub(phi) + k*lap2(phi)
    phit = phi + dt*(pinc) + g
    phi = phi + dt*(pinc + phit - phicub(phit) + k*lap2(phit))/2
    return phi + g

def phip(x):
    ''' derivative of kink shape function '''
    return 1.0/(np.cosh(x/np.sqrt(2)))**2

def separation(i,ii):
    ''' modulus N '''
    j = abs(i-ii)
    if j > N/2:
        j = N-j
    return j

def makeh():
    ''' h(x) is smoothed version of phi(x) '''
    phipl = [phip(i*dx) for i in range(N)]
    h = []
    w = int(30/dx) # width for integration
    for i in range(N):
        h.append(sum([phi[ii%N]*phipl[separation(i,ii)] for ii in range(i-w,i+w)]))
    return [hh*dx*np.sqrt(2)/4 for hh in h]

def cx(phi,i):
```

```python
        ''' sum of product of phi(x) and phi(x+i) '''
        return np.sum(phi*np.roll(phi,i))


pid = os.getpid()
sdt,sdx = str(int(dt*10000)),str(int(dx*100))
stm,sL = str(int(tmax/1000)),str(int(N*dx/1000))
sfname = 'Phis'+str(int(beta))+'_'+str(pid)+'_'+sdx+'_'+sdt+'_'+stm+'.dat'
sfile = open(sfname,'w')
lfname = 'Length'+str(int(beta))+'_'+str(pid)+'_'+sdx+'_'+sdt+'_'+stm+'_'+sL+'.dat'
lfile = open(lfname,'w')
cfname = 'Config'+str(int(beta))+'_'+str(pid)+'_'+sdx+'_'+sdt+'_'+stm+'.dat'
cfile = open(cfname,'w')

def writestuff(sum2,num2,sumc,sumhist):
    '''write to files'''
    h = makeh()
    nk = len([i for i in range(N-1) if h[i]*h[i+1]<0])
    print(int(t+0.4),nk,len([i for i in range(N-1) if phi[i]*phi[i+1]<0]))
    sfile.write('%f\n'%(sum2/num2))
    lfile.write('%.0f_%.2f_%.2f_%i\n'%(t,np.mean(-dxc/np.diff(np.log(sumc))),
                np.std(-dxc/np.diff(np.log(sumc))),nk))
    sum2,num2 = 0.0,0
    sumc,sumhist = np.zeros(len(ilist)),np.zeros(len(thishist))
    ttt = dt/100
    for thisfile in (sfile,lfile,cfile):
        thisfile.flush()

host = os.getenv('HOSTNAME').split('.')[0]
print('N_=', N,'tmax_=', tmax)
print('dx_=', dx,'dt_=', dt,'beta_=',beta)
sfile.write("#_%i_%.0f_%.4f_%.5f_%s\n"%(N,tmax,dx,dt,host))
lfile.write("#_%i_%.0f_%.2f_%s\n"%(N,tmax,tint,host))
xmin,xmax = 10.0,40.0
di,dxc = int(1.0/dx),int(1.0/dx)*dx
ilist = []
i = int(xmin/dx)+1
while i*dx < xmax:
    ilist.append(i)
    i += di

mybins=np.linspace(-2.0,2.0,401,endpoint=True)
tt,ttt = dt/100,dt/100
sum2,num2 = 0.0,0
sumc,sumhist = np.zeros(len(ilist)),np.zeros(len(mybins)-1)

############## main loop ################################
while t < tmax-dt:
    g = myra2(N,fac)
    phi = heun2(phi,g,dt,k)
    t += dt
    tt += dt
    if tt > tint:
        tt = dt/100
        if t > tstart:
            thissums = np.sum(phi*phi)
            sum2 += thissums/N
            num2 += 1
            for i in range(len(ilist)):
                sumc[i]+=cx(phi,ilist[i])/thissums
            ttt += tint
            thishist=np.histogram(phi,bins=mybins,normed=True)[0]
            sumhist += thishist
            writestuff(sum2,num2,sumc,sumhist)
        else:
            print(int(t+0.4),len([i for i in range(N-1) if phi[i]*phi[i+1]<0]))
#########################################################

for i in range(N):
    cfile.write('_%.3f'%phi[i])
for thisfile in (sfile,lfile,cfile):
    thisfile.close
```